

Optimal Operation of Battery Energy Storage System Considering Distribution System Uncertainty

Yu Zheng, *Member, IEEE*, Junhua Zhao, *Senior Member, IEEE*, Yue Song, *Student Member, IEEE*, Fengji Luo, *Member, IEEE*, Ke Meng, *Member, IEEE*, Jing Qiu, *Member, IEEE*, David J. Hill, *Life Fellow, IEEE*

Abstract—We present a novel control strategy of charging and discharging batteries in a distribution system to optimize the energy transaction cost. With an increased proportion of renewable energy in a distribution system, the real demand curve may significantly deviate from the forecast curve, which can lead to an increased challenge for an energy distribution company in making an effective purchase plan. The proposed strategy aims at tracking the total forecast demand curve, and can mitigate risk and encourage demand-side bidding. In this paper, short-term load forecasting, wind power forecasting, and solar power forecasting are performed. To optimize profit, the optimal operation of energy storage systems in a distribution system was developed and solved in a two-level framework considering forecast uncertainties in day-ahead operation and mitigating the net demand gap in real-time operation. To quantify the risk mitigation and profits, the purchase strategies for uncertain and certain demand that occurs the next day were compared. The promising results show that optimal operation of a battery energy storage system can reduce the energy cost and the transaction risk for an energy distribution company.

Index Terms—Operation Strategy, Distribution System, Electricity Markets, Energy Storage System, Renewable Energy

I. INTRODUCTION

WITH the growing proportion of renewable energy and the prevalence of distributed generation, energy distribution companies (DISCOs) are facing new challenges. As an owner and operator of a distribution system, DISCO can buy energy through a pool market or via bilateral contracts to meet the future electricity requirements of end customers [1]-[3]. If DISCOs possess renewable energy facilities and battery energy storage system (BESS), they will have more options for energy acquisition. Moreover, DISCOs can also improve their response capabilities towards the electricity market by optimizing financial bids with efficient BESS operation [4]. Therefore, although DISCOs struggle with the growing complexity presented by the integration of more renewable resources, there are also new economic opportunities in electricity markets that are increased by the ability to provide auxiliary services with BESS.

In distribution systems, battery energy storage can be applied for frequency regulation and peak shaving [5]. For example, Q. Li et al. used a battery system to alleviate detrimental impacts of high penetration solar power [6]. Some researchers have proposed a charging/discharging method of BESS for energy management [7]-[9]. However, these works did not consider market effects into the BESS operation model. Participating in the electricity market with optimal BESS operation is an attractive option, but more research is required to determine the best strategy to maximize profits. Giuntoli and Poli [10] proposed a day-ahead scheduling model for a large-scale virtual power plant (VPP) that contains many small-scale ‘prosumers (producers and consumers)’ and energy storage devices. Aloini et al. [11] proposed an alternate power-scheduling approach for the VPP. Although there have been studies on the operation and control strategies of small-scale market participants, the majority of previous studies focused on VPP but neglected system power loss. With the further development of electricity markets, there is increasing research focus on strategies for DISCOs. J.M. Lujano-Rojas et al. proposed a comprehensive method to optimize the operation of BESS under dynamic pricing schemes in a distribution system [12], but the uncertainties of the renewable power output and real-time electricity were not considered and the network model and system constraints were relaxed for fast real-time optimization, which may lead to inaccurate results. Forecast error-modelling methods are proposed for different distributed resources [14]-[17]. Further, recent advances in the convex relaxation of the optimal power flow (OPF) problem and exact relaxation conditions were summarized by S.H. Low [18][19]. This relaxation method can obtain a globally optimal solution of the original problem with high computation speed, especially for distribution systems where relaxation can be easily achieved. Therefore, we can develop a novel BESS operation framework for a distribution operator to optimize energy transaction cost.

In our previous work, we proposed a novel control strategy to charge and discharge batteries in a distribution system and optimize the allocation of the energy storage system (ESS), especially a battery energy storage system (BESS)[4][13]. To further extend the operation model considering forecast uncertainties and real-time operation, a comprehensive operation framework is proposed in this work. The day-ahead bidding model depends on the accuracy of forecasted information. The key issues for real-time optimal BESS operation are optimization accuracy and speed. The major contribution of this work is to propose an optimal operation framework for DISCO including day-ahead bidding strategy and real-time BESS operation. In the first stage, a stochastic bidding model is used to determine the optimal bid powers

Manuscript received xx. xx, 2017. This work was supported by Hong Kong RGC Theme Based Research Scheme (Grant No. T23-701/14N).

Y. Zheng, David J. Hill and Y. Song are with the Department of Electrical and Electronic Engineering, The University of Hong Kong, Hong Kong (e-mail: zhy9639@hotmail.com, dhill@eee.hku.hk, yuesong@eee.hku.hk).

David J. Hill, F. Luo and K. Meng are with the School of Electrical and Information Engineering, the University of Sydney, Sydney, 2006, NSW Australia (email: dhill@sydney.edu.au, fengji.luo@sydney.edu.au, ke.meng@sydney.edu.au).

J. Zhao is with the School of Science and Engineering, Chinese University of Hong Kong, Shenzhen, China (email: fuxiharp@gmail.com).

required to maximize the DISCO expected profit. In this step, the uncertainties of the VPP's power outputs, profit from spot market, and imbalance costs are considered. In the second stage, a real-time BESS dispatch model is proposed to optimally apply the battery reserve to minimize the DISCO operational cost. A recently developed heuristic optimization method, the natural aggregation algorithm (NAA) [20][21], is employed to solve the day-ahead bidding model. Then, the second-order conic relaxation technique is used to obtain a computationally feasible convex reformulation of the originally nonconvex, real time BESS operation problem. Overall, the proposed operation framework allows optimal scheduling of BESS utilization to optimize DISCO profits with consideration of network constraints and multiple uncertainties.

This paper is organized as follows. After the introduction, an optimal BESS operation framework for energy acquisition of DISCO is presented, and multiple forecast errors are discussed. Next, the day-ahead optimal bidding model and real-time BESS operation model are proposed to reduce DISCO operation cost. After that, the corresponding solving algorithms are introduced for the proposed operation models. The proposed bidding strategy and BESS operation method are then verified on a modified IEEE 15-bus distribution network, and the energy transaction cost is also quantified. Finally, conclusions and further developments are discussed in the last section.

II. OPERATION MODEL OF DISCOS

A. Energy Acquisition Model of DISCOs

The electricity transaction between a generation company and a DISCO can be achieved through a pool market or bilateral contracts. In spot markets, the producers and purchasers bid or negotiate in a day-ahead market, and then the dispatchable power is balanced in the real-time market for each time interval of a day [22]. The real-time prices are formulated according to the type of market. In a deregulated market, the real-time prices are set according to the bids of market participants, and in a regulated market, purchasers trade the energy difference between the real and the expected load at a regulated price [23]. Not matter in which market, the purchasers would be punished if the energy consumption deviates the bidding energy. Based on the net demand forecast and BESS dispatching, DISCOs can save significant energy purchasing cost and reduce the risk arising from operation in both regulated and de-regulated markets by adjusting BESS operation. In this paper, a BESS-based operational model for DISCOs is proposed, as shown in Fig. 1. This model considers different renewable distributed generation units and BESSs within the DISCO control area. In the day-ahead operation model, an optimal bidding strategy considers both forecasted system information and BESS capability. Taking the forecast uncertainties into account of day-ahead bidding model prevents the overuse of BESS and reduces the transaction risk in the electricity market. Additionally, the BESS capacity reserve provides operational flexibility and net demand compensation for real-time operation. The BESS operation strategy is not actually implemented in day-ahead operation scheme, the real time operation module is proposed to

determine the real operation strategy of BESS. The adaption cost is quantified in the proposed method to reserve a fraction of the BESS capacity to compensate for the gap between the real-time demand and the forecasted demand, i.e., power balancing service. Such BESS capacity reserve can be applied to other applications according to the market mechanism.

Consider a radial distribution system comprising N nodes collected in the set $\mathcal{N} := \{1, 2, \dots, N\}$ and overhead lines represented by the set of edges $E := \{(i, j)\} \subset \mathcal{N} \times \mathcal{N}$. Node 1 is taken as the secondary of the step-down transformer. Let $\mathcal{H} \subset \mathcal{N}$ collect nodes that correspond to the buses with BESS. In the day-ahead operation module, the planning time horizon is $\mathcal{T}_D := \{1, 2, \dots, T\}$ with the time interval Δt_d . In this work, the day-ahead planning time horizon T is 24 hours and the time interval Δt_d is 1 hour. In the real-time operation module, the BESS optimal operation problem is developed for each hour with the shot time interval Δt_r . At hour t , we define the real-time planning horizon $\mathcal{T}_t := \{1, 2, \dots, K\}$. Normally, we use 4 15-minute operation time intervals for an hour.

The fluctuating nature of renewable energy (RE) means that the resulting net load profile is very different than the underlying demand profile alone. The effect of RE is to alter the regular nature of the standard demand profile and replace it with a highly variable modified pattern. The net demand can be computed as:

$$P_{Net,i}^t = P_{Load,i}^t - P_{Solar,i}^t - P_{Wind,i}^t \quad (1)$$

$$P_i^t = P_{Net,i}^t + P_{bess,i}^t \quad (2)$$

where t and $_i$ denote the variable at time t and bus i , respectively. $P_{Net,i}^t$, $P_{Solar,i}^t$, $P_{Wind,i}^t$, $P_{Load,i}^t$, $P_{bess,i}^t$, and P_i^t represent the net demand, solar power output, wind power output, load consumption power, BESS charging/discharging power, and total power consumption/generation, respectively at time t bus i .

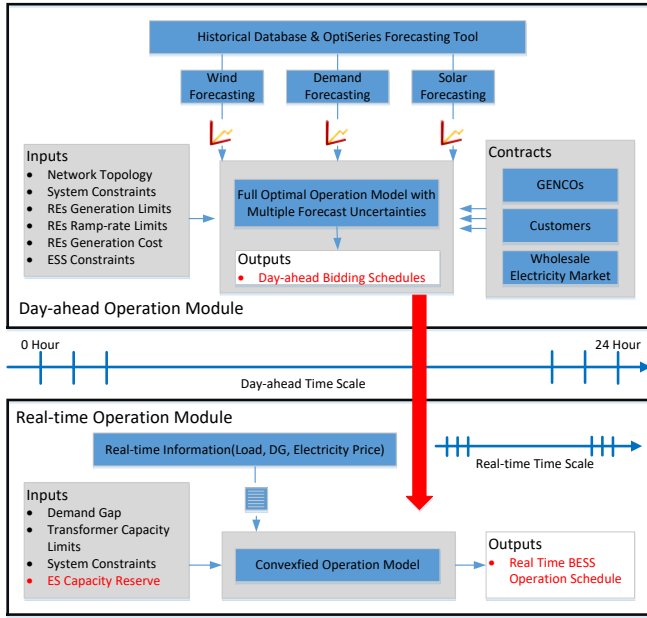


Fig. 1. Proposed operation framework for DISCOs

B. Forecast uncertainties

Forecasting plays a key role in the planning and operation of a distribution system. Due to the uncertainties of renewable energy and the electricity market, the day-ahead net demand and electricity price are unable to be forecasted with high accuracy [24]. As a result, the DISCO must take forecast errors into account in the day-ahead energy-bidding problem. We constructed possible scenarios based on the forecast error probability distribution function (PDF). The scenario is generated randomly from the corresponding PDF of the forecast results. In this approach, a Monte Carlo-based approach can be used to simulate these uncertain renewable outputs and construct the scenarios randomly. For each candidate plan, Monte Carlo simulation is applied to produce a large number of scenarios that incorporate multiple kinds of forecasted data. The different PDFs of forecast errors are discussed as follows.

➤ Wind speed

Research has shown that a two-parameter Weibull probability distribution function matches the random characteristic of wind speed closely. Its probability density function is given as:

$$f_v(v) = \frac{k_v}{c_v} \left[\frac{v}{c_v} \right]^{k_v-1} \exp \left[- \left(\frac{v}{c_v} \right)^{k_v} \right] \quad (3)$$

Given the probability of the wind speed forecast error, the wind power distribution is acquired [17]. The linear transformation is described as,

$$f_w(w) = f_v \left(\frac{w-b_w}{a_w} \right) \left| \frac{1}{a_w} \right| \quad (4)$$

where, $f_v(v)$ and $f_w(w)$ are the forecast error probability density function (PDF) of wind speed and wind power, respectively; w is the wind power and v is the wind speed. $k_v, c_v, a_w,$ and b_w are all variables of the probability function.

➤ Solar forecast uncertainty

The uncertainty of solar radiation mainly comes from the stochastic nature of weather conditions that determine the cloudiness or clearness, allowing different amounts of solar radiation to be captured. Therefore, a clearness index is adopted to address this problem. The random behavior of the clearness index is expressed by a Beta distribution function.

$$f_{cl}(k_t) = \frac{\Gamma(a_k + b_k)}{\Gamma(a_k)\Gamma(b_k)} k_t^{a_k-1} \cdot (1-k_t)^{b_k-1} \quad (5)$$

where, $f_{cl}(k_t)$ is the PDF of the clearness index; k_t is the clearness, and a_k and b_k are the Beta parameters.

➤ Load forecast uncertainty

A Gaussian distribution $f_l(l)$ is used in this paper to statistically model the load forecast error. The pdf for a Gaussian distribution is:

$$f_l(l) = \frac{1}{\sqrt{2\pi\sigma_l^2}} \exp \left[- \frac{(l-\mu_l)^2}{2\pi\sigma_l^2} \right] \quad (6)$$

where, μ_l and σ_l are the statistical mean and standard deviation of the load demand.

➤ Electricity Price Uncertainty

The electricity price forecast error is also modeled by a Gaussian distribution as

$$f_p(p) = \frac{1}{\sqrt{2\pi\sigma_p^2}} \exp \left[- \frac{(p-\mu_p)^2}{2\pi\sigma_p^2} \right] \quad (7)$$

where, $f_p(p)$ is the PDF of the electricity price, μ_p and σ_p are the statistical mean and standard deviation of the load demand.

C. Day-ahead Optimal Bidding Model

Note that in the deregulated market, the day-ahead energy procurement prices and quantities are usually fixed as a result of a price clearing procedure. According to the nature of each market, we assume that there is no market power that can affect the pool prices in a deregulated market. The optimization goal of the day-ahead problem is to minimize the overall system operation cost in supplying the net demand. As stated by our previous work, the optimal operation of BESS can help DISCO reduce the energy procurement cost in the day-ahead market by charging when prices are low and then discharging when the prices are high. Considering forecast uncertainties, the day-ahead bidding model is represented by

$$\begin{aligned} \min J_1 &= \sum_{s=1}^{n_s} \sum_{t=1}^T \left\{ \lambda^t \cdot \bar{P}_{bid}^t \cdot \Delta t_d + \sum_{i \in \mathcal{H}} C_{bess} (P_{bess,i}^t, \Delta t_d) + C_a^{t,s} \right\} \\ &= \sum_{t=1}^T \lambda^t \cdot \bar{P}_{bid}^t \cdot \Delta t_d + \sum_{t=1}^T \sum_{i \in \mathcal{H}} C_{bess} (P_{bess,i}^t, \Delta t_d) + \frac{1}{S} \cdot \sum_{s=1}^S \sum_{t=1}^T C_a^{t,s} \end{aligned} \quad (8)$$

where s denotes the variable in scenario s , the total scenario number is n_s , and Δt_d is the optimization time interval. In eq.(8), the first term represents the bidding cost in the energy market, the second term is the BESS operation cost C_{bess} , and the third term denotes the adaption cost to compensate for forecast errors in scenario s . The decision variables include the bid capacity $P_{bid}^t, t \in \mathcal{T}_D$ and the BESS charging/discharging schedule $P_{bess,i}^t, i \in \mathcal{H}, t \in \mathcal{T}_D$. The normal bidding amount depends on the expected total net

demand at the substation, namely $P_{bid}^t = P_1^t$. P_1^t is obtained by calculating the system power flow including BESS charging/discharging and based on forecasted information. In day-ahead operation, the solar output, wind output, demand, and electricity price are forecasted as $\bar{P}_{Solar,i}^t, \bar{P}_{Wind,i}^t, \bar{P}_{Load,i}^t$, and $\bar{\lambda}^t$. We generated different scenarios for the day-ahead operation model. In each scenario, the errors of renewable energy output, demand, and electricity price are sampled from the forecast error distribution function described in the above section. We define $P_{Solar,i}^{t,s}, P_{Wind,i}^{t,s}, P_{Load,i}^{t,s}$, and $\lambda^{t,s}$ for scenario s and the net demand as $P_{Net,i}^{t,s}$. The adaption cost $C_a^{t,s}$ in a scenario represents the punishment cost for constraint violations and transaction loss in the electricity market for that scenario [25][26]. If the BESS can compensate for the demand gap and mitigating constraint violations of scenario s , the adaption cost is calculated by the BESS operation cost. Otherwise, a transaction punishment from the market and a constraint violation cost is added to the adaption cost.

The battery operation cost can be represented by

$$C_{bess} (P_{bess,i}^t, \Delta t) = \lambda_{fix} \cdot \Delta t + \lambda_{cha} (1 + \eta_c) \cdot |P_{bess,i}^t| \cdot \Delta t \quad (9)$$

where λ_{fix} is the hourly fixed battery operation cost (\$/h) which covers the investment of inverter and other hardware; λ_{cha} is the battery charging/discharging cost parameter (\$/kWh) which is converted from battery degradation. Due to the effect of discharge rate on battery life [27], the total energy charging/discharging capability of battery remains stable within a reasonable depth of discharge (DOD). As such, the charging/discharging cost is nearly proportional to the power rating and the capacity rating of the battery. λ_{cha} can be calculated by dividing battery cost by total energy charging/discharging capability. η_c is the charging efficiency (%).

The day-ahead bidding model is subjected to the following constraints:

$$\text{for } i \in \mathcal{H}, t \in \mathcal{T}_D,$$

➤ **BESS Constraints**

The state of ESS, the key issue for battery control strategy, can be described as,

$$\Delta S_i^t = \Delta t P_{bess,i}^t - \eta_c |P_{bess,i}^t| \cdot \Delta t - \eta_{loss} S_i^t \quad (10)$$

where η_{loss} is the leakage loss factor (%).

The state-of-charge (SOC) is expressed as follows,

$$SOC_i^t = S_i^t / S_i^{ra} \quad (11)$$

$$\text{Daily operation constraint: } SOC_i^{24} = SOC_i^1 \quad (12)$$

$$\text{Power limits: } P_{bess,i}^{Dis,Max} \leq P_{bess,i}^t \leq P_{bess,i}^{Chr,Max} \quad (13)$$

$$\text{SOC limits: } SOC_i^{Min} \leq SOC_i^t \leq SOC_i^{Max} \quad (14)$$

where ΔS_i^t , S_i^t , S_i^{ra} and SOC_i^t are the charging energy, energy in battery, energy capacity, and state-of-charge of BESS, respectively, at bus i and time t . $P_{bess,i}^{Dis,Max} / P_{bess,i}^{Chr,Max}$ and SOC_i^{Min}

SOC_i^{Max} represent the charging power and SOC constraints.

$$\text{for } \forall i \in \mathcal{N} \setminus \{1\}, t \in \mathcal{T}_D,$$

➤ **Power balance constraint**

$$V_i^t \sum_{j=1}^n Y_{ij}^* (V_j^t)^* = P_{bess,i}^t - P_{Net,i}^{t,s} - j \cdot Q_{Net,i}^{t,s} \quad (15)$$

where, the superscript * means conjugate.

➤ **Voltage constraint**

The voltage magnitude of each node must lie within their power quality limitation.

$$V_i^{\min} \leq |V_i^t| \leq V_i^{\max} \quad (16)$$

➤ **Current constraint**

The current magnitude of each branch must be lower than the rating current to ensure cable thermal stability.

$$|I_{ij}^t| < I_{ij}^{\max} \quad (17)$$

➤ **Power source limit constraint**

Dispatch power and reverse power flow through the substation transformer is allowed within the limitation of the transformers' capacity and protection system constraints.

$$|P_i^t| \leq S_{TR}^{\max} \quad (18)$$

where V_i^t, V_i^{\min} , and V_i^{\max} are the voltage of bus i at time t and the maximum and minimum voltage magnitude limit. Y_{ij} and I_{ij}^{\max} are the admittance and current limit of line ij . I_{ij}^t is the current through line ij . S_{TR}^{\max} is the rating dispatch power of the distribution station.

D. Real-Time Optimal BESS Operation

By solving the model in (8), the DISCO determines the optimal bids. The BESS reference operation schedules are determined accordingly in the day-ahead stage. With the consideration of the adaption cost in the day-ahead BESS operation schedule model, the resulting power and SOC of BESS will maintain an optimal reserve to deal with the potential risk in the electricity market. In the real-time stage, the DISCO updates the real-time information and the BESS capacity reserves to optimize the actual BESS operation schedule based on real-time information. The real-time operation is with a shorter time interval (one to several minutes) than the day-ahead bidding interval (e.g. hourly-based). Therefore, the optimization problem should be solved frequently and at a fast speed. A BESS operation model is proposed for DISCO and transformed to a convex problem to implement real-time fast optimization. The real-time operation provides multiple benefits to the DISCO, including a more flexible BESS operation strategy that can quickly respond to real time information, exploiting the potential BESS capacity reserve, and power loss saving with a shorter operation interval. The real time information can be predicted with high accuracy. Without forecast uncertainties, the problem is formulated as follows:

$$\min J_2 = \sum_{t_k \in \mathcal{T}_t} \left\{ \lambda_p \cdot (\bar{P}_{bid}^t - P_1^k) \Delta t_r + \sum_{i \in \mathcal{H}} C_{bess} (P_{bess,i}^k) \right\} \quad (19a)$$

$$\text{s.t. for } \forall i \in \mathcal{N} \setminus \{1\}, t_k \in \mathcal{T}_t,$$

$$V_i^{t_k} \sum_{j=1}^n Y_{ij}^* (V_j^{t_k})^* = P_{bess,i}^{t_k} - P_{Net,i}^{t_k} - j \cdot Q_{L,i}^{t_k} \quad (19b)$$

$$V_i^{\min} \leq |V_i^{t_k}| \leq V_i^{\max} \quad (19c)$$

$$P_{bess,i}^{Dis,Max} \leq P_{bess,i}^{t_k} \leq P_{bess,i}^{Chr,Max} \quad (19d)$$

$$SOC_i^{Min} \leq SOC_i^{t_k} \leq SOC_i^{Max} \quad (19e)$$

$$|I_{ij}^{t_k}| < I_{ij}^{\max} \quad (19f)$$

$$|P_i^{t_k}| < S_{TR}^{\max} \quad (19g)$$

The objective is to minimize the real time energy gap and battery operation cost where power loss reduction is implied. Within each dispatch horizon, i.e. 1 hour, the optimal charging dispatch schedules for every real-time operation interval Δt_r , i.e. 15 mins, can be acquired by solving the problem (19).

III. OPTIMIZER

A. Approach to solve the bidding model

The day-ahead bidding model is a nonlinear, constrained mixed-integer programming problem, which is difficult to solve by mathematical programming methods. This paper uses a new evolution algorithm, NAA, to solve the proposed model. Unlike other EAs, NAA distributes individuals to several sub-populations (called ‘shelters’), and uses a stochastic migration model to dynamically mitigate the individuals among the shelters. The inter-individual at-traction effect and crowding effect are considered in the migration model to balance exploration and exploitation. The key operators of NAA are briefly introduced below.

Step 0: Input data

Input the simulation data, such as network, renewable generation, load, and price information

Step 1: Population Initialization

In NAA, each individual representing an BESS operation schedules in the population with the size is coded as a 72-dimensional vector (24 hours charging/discharging power of 3 BESS). For each individual, its initial value is randomly generated within the initial bounds.

Step 2: Shelter Initialization

In NAA, each sub-population is called a ‘shelter.’ After generating the populations, the fitness value of each individual is evaluated by calculating eq. (8). The individuals with minimum fitness values are selected as the shelter leaders, and are associated with the shelter indexes. The positions of the shelter leaders become the shelter sites. The rest of the individuals are sequentially distributed to each shelter, and are associated to corresponding shelter indexes.

Step 3: Stochastic Migration Model

In each generation, each individual of the population makes a decision about leaving or entering a certain shelter [20].

Step 3.1: Decision Making of Exploit Individual

Each individual evaluates its probability of leaving its current shelter and makes decision.

Step 3.2: Decision Making of an Explorer Individual

The explore individual randomly selects a shelter, evaluates the entering probability, and then makes a decision.

Step 4: Located Search

If an exploit individual is a shelter leader, it tries to search its neighbored area and perform a crossover to generate a new

candidate.

Step 5: Generalized Search

Each explore individual randomly selects two different individuals to generate a mutant and perform the crossover operation.

Step 6: Selection & Termination

At the end of each generation, the individuals are sorted in the ascendant order and shelter leaders are updated. The algorithm terminates when the maximum generation time is reached.

B. Approach to solve the real-time operation model

The problem (19) is generally non-convex due to the power flow constraints (19b), which makes it difficult to guarantee the global optimality of the solution. Next we will introduce some relaxation techniques to convexify the original problem. Let $\mathbf{W}^{t_k} \in \mathcal{C}^{m \times n}$, $t_k \in \mathcal{T}_t$ be a matrix defined by the distribution network in t -th time slot, whose entries take values as $W_{ij}^{t_k} = |V_i^{t_k}|^2$ for $i = j$, $W_{ij}^{t_k} = V_i^{t_k} (V_j^{t_k})^*$ for $i \neq j$, $Y_{ij} \neq 0$ and $W_{ij}^{t_k} = 0$ otherwise. There are a total of $2n - 1$ non-zero entries in \mathbf{W}^{t_k} as the distribution network is radial. Denote

$$P_i(\mathbf{W}^{t_k}) = \text{Re} \left\{ Y_{ii}^* W_{ii}^{t_k} + \sum_{Y_{ij} \neq 0} Y_{ij}^* W_{ij}^{t_k} \right\} \quad (20a)$$

$$Q_i(\mathbf{W}^{t_k}) = \text{Im} \left\{ Y_{ii}^* W_{ii}^{t_k} + \sum_{Y_{ij} \neq 0} Y_{ij}^* W_{ij}^{t_k} \right\} \quad (20b)$$

By taking $\mathbf{W}^t, t_k \in \mathcal{T}_t$ as the control variable, Eq.(19) can be reformulated as

$$\min \sum_{t_k \in \mathcal{T}_t} \left\{ \lambda_p \cdot (\bar{P}_{bid}^t - P_1(\mathbf{W}^{t_k}) \cdot \Delta t_r) \right. \quad (21a)$$

$$\left. + \sum_{i \in \mathcal{H}} C_{bess} (P_i(\mathbf{W}^{t_k}) - P_{Net,i}^{t_k}) \right\}$$

$$s.t. \text{ for } \forall i \in \mathcal{N} \setminus \{1\}, t_k \in \mathcal{T}_t,$$

$$P_{Net,i}^{t_k} + P_{bess,i}^{Dis,Max} \leq P_i(\mathbf{W}^{t_k}) \leq P_{Net,i}^{t_k} + P_{bess,i}^{Chr,Max} \quad (21b)$$

$$Q_i(\mathbf{W}^{t_k}) = -Q_{Net,i}^{t_k} \quad (21c)$$

$$|I_{ij}^{t_k}| < I_{ij}^{\max} \quad (21d)$$

$$P_i(\mathbf{W}^{t_k}) < S_{TR}^{\max} \quad (21e)$$

$$(V_i^{\min})^2 \leq |W_{ii}^{t_k}| \leq (V_i^{\max})^2 \quad (21f)$$

$$SOC_i^{Min} \leq SOC_i^{t_k} \leq SOC_i^{Max} \quad (21g)$$

$$\sum_{k=1}^s P_i(\mathbf{W}^{t_{c+k-1}}) - E_i^{t_s} \leq D_{H,i}, \forall i \in \mathcal{H}, s \in \mathcal{S}, \quad (21h)$$

$$W_{ii}^{t_k} W_{jj}^{t_k} \geq |W_{ij}^{t_k}|^2, \forall Y_{ij} \neq 0 \quad (21i)$$

$$\text{rank} \left(\begin{bmatrix} W_{ii}^{t_k} & W_{ij}^{t_k} \\ W_{ij}^{t_k} & W_{jj}^{t_k} \end{bmatrix} \right) = 1, \forall Y_{ij} \neq 0 \quad (21j)$$

where $SOC_i^{t_k}$ can be written as a linear function of \mathbf{W}^t . Equations (21b) ~ (21e) are power flow constraints, (21f) shows the voltage magnitude constraints, and (21g) and (21h) are charging constraints.

Since (21b) ~ (21h) are linear in terms of \mathbf{W}^t and (21i) is a second-order cone constraint, the problem (21) is indeed convex if the rank constraint (21j) is dropped. Such relaxation is exact for radial networks with non-heavy power flow across lines [18], which holds for most normal operation modes in distribution networks, so that the globally optimal charging schedule $P_{bess,i}^{t_k}, i \in \mathcal{H}, t_k \in \mathcal{T}_t$ can be recovered from $\mathbf{W}^{t_k}, t_k \in \mathcal{T}_t$ by

$$P_{bess,i}^{t_k} = P_{Net,i}^{t_k} - P_i(\mathbf{W}^t). \quad (22)$$

IV. CASE STUDY

A. IEEE 15-bus system

One modified IEEE 11kV, 15-bus distribution radial system was used to verify the proposed ESS allocation approach. The benchmark system consists of fourteen loads, two wind farms, and one solar station. The 850kW wind farm is installed at the bus 11 and the 800kW wind farm is located at bus 9. The solar farm is constructed at bus 6. The one-line diagram of this distribution system is shown in Fig. 2. The historical wind and solar data were obtained from two observation stations in Australia. The electricity price data was taken from the PJM website [29]. The forecasted 24-hour net demand profile and day-ahead electricity price are shown in Fig. 3. With the integration of renewable energy, the demand peak is located at a lower price time interval and the energy cost is reduced. Moreover, the operation of BESS provides the opportunity to purchase more energy at a lower price and sell the energy back to the main grid at a higher price, and mitigates the transaction risk caused by multiple uncertainties.

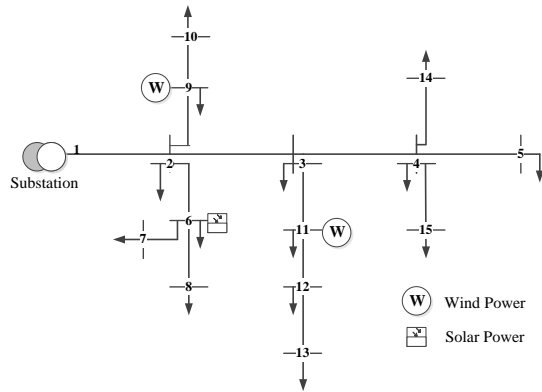


Fig. 2. Modified IEEE 15-bus distribution radial system

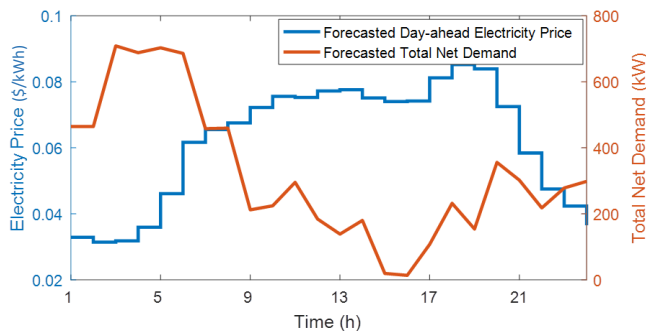


Fig. 3. Forecasted hourly net demand profiles of the buses with renewable energy

We assume BESSs are located at the distributed renewable generation site and the parameters are listed in Table I [30]. The optimal operation schedule of BESS in the day-ahead operation framework is to minimize the energy cost of purchasing energy from main grid. If the day-ahead forecast is accurate, the whole BESS capacity can be applied to store energy when the price is low and release back when the price is high. We define this BESS operation method as the reference strategy. The charging/discharging schedules in this scenario are shown in Fig. 4. The SOC of the BESSs are shown in Fig. 5.

TABLE I
TYPICAL PARAMETERS OF LEAD-ACID BATTERY

Item	Lead-acid Battery		
Location	6	9	11
S_i^{ra} (kWh)	500	500	500
$P_{bess,i}^{Chr,Max} / P_{bess,i}^{Dis,Max}$ (kW)	200/-200	200/-200	200/-200
SOC^{max} / SOC^{min}	0.9/0.2		
Life Cycle	1000 times		
$\lambda_{fix} \lambda_{cha} \eta_c \eta_{loss}$	0.025\$/h; 4.69\$/kWh; 95%; 3% per month		

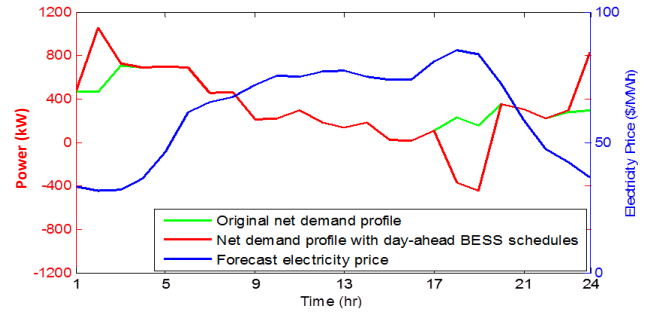


Fig. 4. Day-ahead BESS schedules of the reference strategy

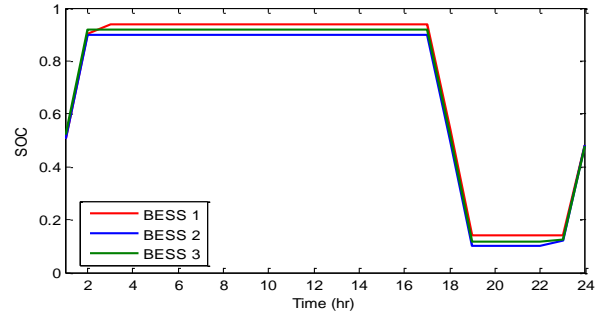


Fig. 5. Day-ahead scheduled SOC of the BESSs with the reference strategy

By using this strategy, the BESSs are charging and discharging with maximum capacity one time per day. As the SOC constraints are reached, the BESS cannot be reserved for other applications. The bidding amount of DISCO in the day-ahead market follows the net demand profile with the BESS schedule. Although the BESS can reduce energy cost with the reference strategy in power market, the DISCO still faces a high transaction risk due to forecast error. Therefore, the adaption cost should be quantified in the day-ahead operation scheme to reserve BESS capacity to compensate the gap between the real-time demand and the forecasted demand. Next, we tested the proposed day-ahead optimal BESS scheduling method with uncertainties. We generated the PDFs of forecast errors from historical data and performed a forecast of system for the next day. As shown in Fig. 6, the forecasted net demand profiles of the buses with distributed renewable

generation was plotted with probability distributions.

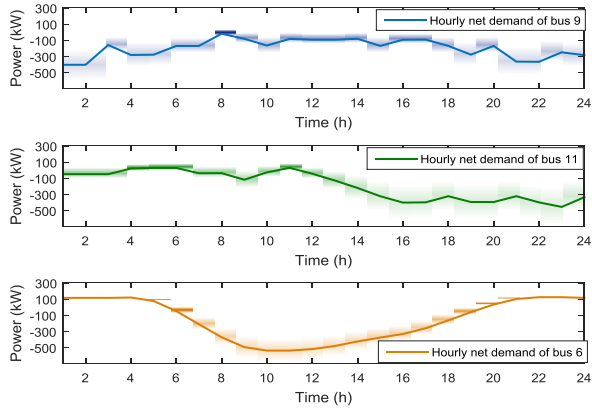


Fig. 6. Forecasted hourly net demand profiles and probability distributions of the buses with renewable energy

The scenarios are constructed by generating the net demands from probability distributions to quantify the adaption cost in the proposed day-ahead bidding model. The proposed day-ahead bidding problem was solved using NAA. The convergence process of the proposed algorithm is shown in Fig. 7 and compared with the differential evolution (DE) and particle swarm optimization (PSO) strategies. The objective value of each possible solution represented by an individual was calculated in different scenarios. The day-ahead bidding results and optimal BESS operation schedules of the proposed strategy are shown in Fig. 8.

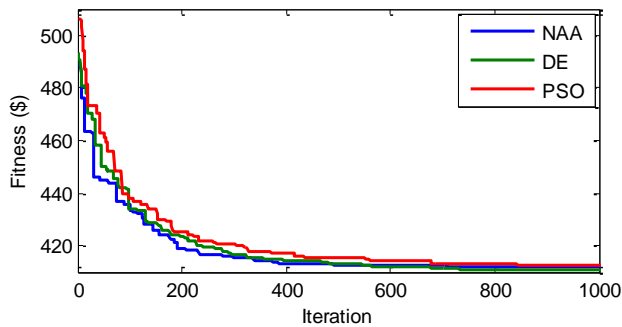


Fig. 7. Convergence processes of different algorithms

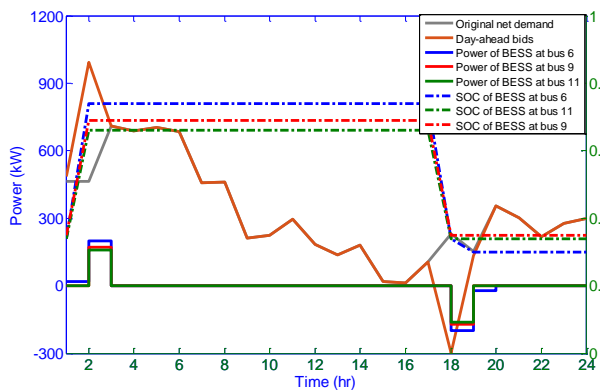


Fig. 8. Day-ahead bidding and BESS schedules with the proposed strategy

As shown in the figure, BESSs are also scheduled to charge at the lowest price time and discharge at the peak price time. A certain part of BESS capacity is reserved for real-time demand gap compensation, and this capacity depends on the forecast

accuracy. The SOC of BESS at bus 6 is deeper than the SOC of BESS at bus 9 and 11, as the forecast error of wind power is larger than solar power. The expected profits of the proposed day-ahead BESS operation strategy and reference strategy are compared in Table II, taking multiple uncertainties into account. It is clear that the transaction risk is reduced significantly by applying the proposed strategy.

TABLE II
COMPARISON OF PROPOSED STRATEGY AND REFERENCE STRATEGY

	Reference strategy	Proposed strategy
Expected total energy cost in day-ahead market (\$)	448.49	433.63
Adaption cost (\$)	38.17	7.25
BESS operation cost (\$)	45.97	29.32
Energy transaction cost (\$)	364.35	397.06

After optimization of the day-ahead BESS operation schedule, the DISCO can bid in the day-ahead market according to the forecast net demand. It should be noted that, the BESS schedule in the day-ahead operation frame is only applied for making bids in the day-ahead market without sending charging/discharging signals to the BESSs. The operation of the BESSs are scheduled and implemented in the real-time operation frame. In real-time operation, problem (19) is solved to mitigate the net demand gap with minimum operation cost, including BESS charging/discharging cost and line loss. For a real-time operation problem, calculation speed is a key issue. As such, a second-order conic relaxation technique is used to obtain a computationally feasible convex reformulation of the originally nonconvex, real time BESS operation problem. The average time consumed is around 0.1second [31] (computing platform: Intel Core i5-4570 CPU 3.20 GHz, RAM 8.00 GB), which allows the online BESS dispatch to track net demand. In this simulation, the real-time data were generated from the PDFs randomly to test the proposed BESS operation method. The minute-based real-time net demand is shown by the blue line in Fig. 9 and compared with day-ahead bids.

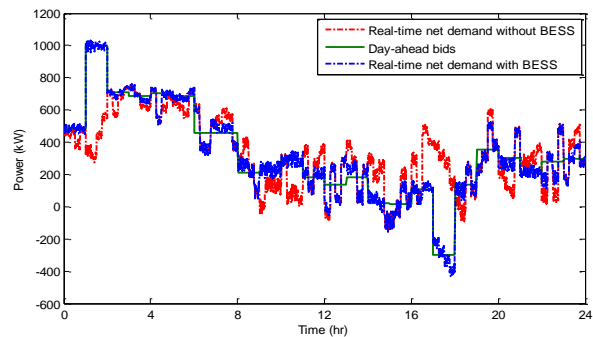


Fig. 9. Real-time net demand with proposed real-time BESS operation strategy (1-min intervals)

Without BESS compensation, real-time net demand deviates significantly from the day-ahead bidding profile and causes a high penalty cost. The real-time net demand with BESS is shown as the red line in Fig. 9. The hourly net demand with BESS is very close to the bidding profile. To show the result more clearly, the 15 minute-based net demand profiles are shown in Fig. 10.

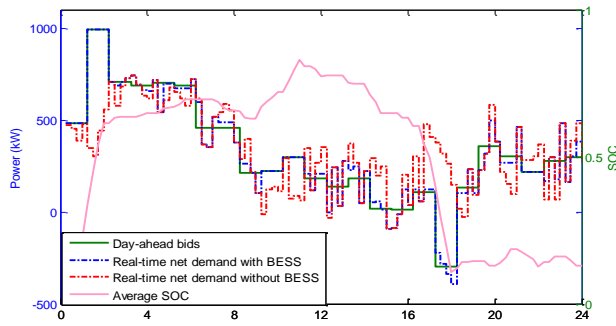


Fig. 10. Real-time net demand with proposed real-time BESS operation strategy (15-min intervals)

The energy transactions are counted hourly. The objective of real-time BESS operation is to compensate the hourly net demand. Therefore, the power can deviate from the bidding profile within an hour. In order to clearly show the charging/discharging power of the three installed ESSs, we present the detailed charging/discharging power of the BESSs over two continuous hours in Fig. 11 and Fig. 12.

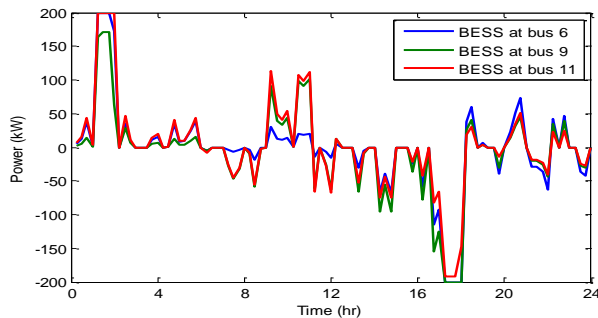


Fig. 11. Real-time BESS charging profiles of a day

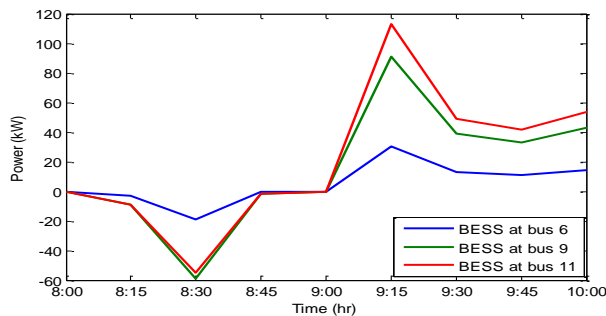


Fig. 12. Real-time BESS charging profiles of two continuous hours (8:00-10:00)

Within a billing period, i.e. 1 hour, the forecasted hourly demand gap is dispatched in four time intervals and three BESSs by solving Eq. (21) for minimum energy cost. From the figure, we see that i) the charging/discharging power of BESS is optimized to mitigate net demand gap; ii) the charging/discharging power of BESS in different time intervals and at different locations is optimized to reduce line loss; iii) the charging states in the four time intervals of a billing period are the same (charging or discharging). The operation benefits and cost are shown in Table III. Two strategies are performed for comparison. In the first strategy, the operator bids according to net demand and operates without BESS. In the second strategy, the operator bids as the proposed day-ahead bidding method and mitigates demand

gap by dispatching BESSs equally and constant power within an hour. From the figure, we can conclude that with the proposed BESS operation method, the distribution company can save the total energy cost.

TABLE III
TOTAL OPERATION COST COMPARISON(\$/DAY)

Energy Transaction Cost	Strategy 1	Strategy 2	Proposed strategy
Day-ahead (bidding cost)	440.25	397.06	397.06
Real-time (BESS operation cost)	0	38.63	33.17
Real-time (balancing cost)	76.34	9.28	8.13
Total cost	537.67	444.97	438.36

B. Sensitivities analysis

In order to show the effectiveness of the proposed method for different BESS capacity and cost, sensitivity analysis was performed as follows:

➤ *BESS Capacity*

To evaluate the impact of BESS capacity on the energy transaction cost, three scenarios were constructed, high BESS capacity, medium BESS capacity, and low BESS capacity. The BESS location and capacity in different scenarios are shown in Table IV. The other parameters are the same as case A. The simulation results under these scenarios are illustrated in Fig. 9. The energy transaction costs are compared in Table V. With advanced forecast technology, the forecast accuracy could be enhanced and the required BESS capacity is reduced accordingly.

TABLE IV
BESS CAPACITY IN DIFFERENT SCENARIOS

Scenario	High	Medium	Low
Bus 6	1000kWh/400kW	500kWh/200kW	250kWh/100kW
Bus 9	1000kWh/400kW	500kWh/200kW	250kWh/100kW
Bus 11	1000kWh/400kW	500kWh/200kW	250kWh/100kW

TABLE V
ENERGY TRANSACTION COST COMPARISONS OF DIFFERENT BESS CAPACITY (\$/DAY)

Energy transaction cost	BESS Capacity Scenario		
	High	Medium (reference)	Low
Day-ahead (Bidding Cost)	357.18	397.06	416.23
Real-time (BESS operation cost)	82.19	33.17	19.23
Real-time (balancing cost)	1.12	8.13	10.18
Total cost	440.49	438.36	445.64

➤ *BESS Cost*

For analysis of the impact of BESS cost and type on the optimal schedule, three BESS types were chosen and the BESS costs were set accordingly. The first two types of BESS are lead-acid battery with different rated charging current (0.5C or 1C), the third BESS is Lithium-Ion with 0.5C charging current. The costs parameter λ_{fix} are 0.025, 0.05, or 0.5 \$/h and the operation costs λ_{cha} are 4.69, 4.69, or 9 \$/kWh. The total energy transaction costs for the different BESS types are compared in Table VI. It is obvious that the BESS cost is a great barrier. Along with development of battery technology, the costs of batteries will decrease, which makes the BESS more feasible to reduce energy transaction risk.

TABLE VI
UTILITY IMPROVEMENT COMPARISONS OF DIFFERENT BATTERY COST (\$/DAY)

Energy Transaction Cost	Battery Cost Scenario		
	lead-acid(0.5C) (reference)	lead-acid(1C)	Lithium-Ion(0.5C)
Day-ahead (bidding cost)	397.06	396.12	405.13

Real-time (BESS operation cost)	33.17	45.98	42.26
Real-time (balancing cost)	8.13	6.55	12.33
Total cost	438.36	448.65	459.72

V. CONCLUSION

This paper proposes a practical two level BESS operation model for DISCOs to reduce the energy cost and the transaction risk. The optimal operation strategy of BESS can help DISCOs make energy purchasing bids in day-ahead market considering uncertainties and implement real-time optimal BESS dispatch to mitigate the risk of the energy trading. Especially in the distribution system with high penetration of renewable energy, the integration of BESS can significantly reduce the energy loss caused by the uncertainty of the demand and distributed generators. The effectiveness of the proposed project has been tested with comprehensive case studies. From the case study results, the overall energy cost is reduce significantly and the transaction risk is effectively mitigated. Further work will consider multiple applications of BESS and multiple BESS aggregators. For multiple applications, we can develop a multi-objective function to exploit more benefits of BESS and study suitable solving algorithms. For multiple BESS owners, game theory can be applied to study the equilibrium operation point.

REFERENCES

[1] J. Momoh, and L. Mili, Economic Market Design and Planning for Electric Power Systems, *Institute of Electrical and Electronics Engineers*.

[2] Y. Liu and X. Guan, "Purchase allocation and demand bidding in electric power markets," *IEEE Trans. Power Syst.*, vol. 18, no. 1, pp. 106-112, Feb. 2003

[3] K. Zare, M. Parsa, and M.K. Sheikh-El-Eslami, "Risk-based electricity procurement for large consumers," *IEEE Trans. Power Syst.*, vol. 26, no. 4, pp. 1826-1834, Nov. 2011.

[4] Y. Zheng, Z. Y. Dong, F. J. Luo, K. Meng, J. Qiu, and K. P. Wong, "Optimal Allocation of Energy Storage System for Risk Mitigation of DISCOs With High Renewable Penetrations," *Power Systems, IEEE Transactions on*, vol. 29, pp. 212-220, 2014.

[5] R. Sebastián, "Application of a battery energy storage for frequency regulation and peak shaving in a wind diesel power system", *IET Gen. Trans. & Dist.*, vol. 10, no. 3, pp. 764-770, 2016.

[6] Q. Li, R. Ayyanar, and V. Vittal, "Convex optimization for DES planning and operation in radial distribution systems with high penetration of photovoltaic resources", *IEEE Trans. Sust. Energy*, vol. 7, no. 3, pp. 985-995, July. 2016.

[7] L. Wang, D.H. Liang, A.F. Crossland, P.C. Taylor, D. Jones, and N.S. Wade, Coordination of multiple energy storage units in a low-voltage distribution network", *IEEE Smart Grid*, vol. 6, no. 6, pp. 2906-2918, Nov. 2015.

[8] W. Shi, X. Xie, C. Chu, and R. Gadh, "Distributed optimal energy management in microgrids", *IEEE Smart Grid*, vol. 6, no. 3, pp. 1137-1146, Nov. 2015.

[9] N. Jayasekara, M.A.S. Masoum, and P.J. Wolfs, "Optimal operation of distributed energy storage systems to improve distribution network load and generation hosting capability" *IEEE Trans. Sust. Energy*, vol. 7, no. 1, pp. 250-261, July. 2016.

[10] M. Giuntoli, D. Poli, "Optimized thermal and electrical scheduling of a large scale virtual power plant in the presence of energy storages", *IEEE Trans. Smart Grid*, vol. 4, no. 2, pp. 942-955, 2013

[11] D. Aloini, E. Crisostomi, M. Raugi, et al., "Optimal power scheduling in a virtual power plant", *Proc. Second IEEE PES Int. Conf. and Exhibition on Innovative Smart Grid Technologies*, 2011

[12] J.M. Lujano-Rojas, R. Dufo-López, J.L. Bernal-Agustín, and J.P.S. Catalán, "Optimizing daily operation of battery energy storage systems under real-time pricing schemes", *IEEE Smart Grid*, vol. 8, no. 1, pp. 316-330, Nov. 2017.

[13] Y. Zheng, Z. Y. Dong, K. Meng, F. J. Luo, H. Q. Tian, and K. P. Wong, "A control strategy of battery energy storage system and allocation in distribution systems," in *Power and Energy Society General Meeting (PES), 2013 IEEE*, 2013, pp. 1-5.

[14] M. R. Patel., *Wind and Solar Power Systems*: CRC Press LLC, 1999.

[15] J. Hetzer, D. C. Yu, and K. Bhattacharai, "An Economic Dispatch Model Incorporating Wind Power," *Energy Conversion, IEEE Transactions on*, vol. 23, pp. 603-611, 2008.

[16] V. A. G. a. K. G. T. Hollands, "A method to generate synthetic hourly solar radiation globally," *Solar Energy*, vol. 44, pp. 333-341, 1990.

[17] Z. Kai, A. P. Agalgaonkar, K. M. Muttaqi, and S. Perera, "Distribution System Planning With Incorporating DG Reactive Capability and System Uncertainties," *Sustainable Energy, IEEE Transactions on*, vol. 3, pp. 112-123, 2012.

[18] S.H. Low, "Convex relaxation of optimal power flow—part I: exactness," *IEEE Trans. Con.. Net. Syst.*, vol. 1, no. 2, pp. 15-27, Jun. 2014.

[19] S.H. Low, "Convex relaxation of optimal power flow—part II: exactness," *IEEE Trans. Con.. Net. Syst.*, vol. 1, no. 2, pp. 177-189, Jun. 2014.

[20] F. Luo, Z.Y. Dong, Y. Chen J. Zhao, "Natural Aggregation Algorithm: A New Efficient Metaheuristic Tool for Power System Optimizations" *IEEE Smartgrid Comm*, Sydney, Australia, 2017.

[21] F. Luo, J. Zhao, and Z.Y. Dong "A New Metaheuristic Algorithm for Real-Parameter Optimization: Natural Aggregation Algorithm", *IEEE Congress on Evolutionary Computation*, 24-29 July, 2016.

[22] J. Zhao, Y. Xu, F. Luo, , et al., "Power system fault diagnosis based on history driven differential evolution and stochastic time domain simulation", *Inf. Sci.*, vol. 275, pp. 13-29, 2014.

[23] Lev S. Belyaev, Electricity market reforms, 2011 by Springer Science and Business Media LCC.

[24] A.L. Ott, "Experience with PJM market operation, system design and implementation," *IEEE Trans. Power Syst.*, vol. 18, no. 2, pp. 528-534, May. 2003.

[25] The *OptiSeries V1.0 User Manual*, PolyU, Sep. 2009.

[26] J.H. Zhao, Z.Y. Dong, P. Lindsay, and K.P. Wong, "Flexible transmission expansion planning with uncertainties in an electricity market," *IEEE Trans. Power Syst.*, vol. 24, no. 1, pp. 479-488, Feb. 2009.

[27] Y. Zheng, Z. Y. Dong, Y. Xu, K. Meng, J.H. Zhao and J. Qiu, "Electric vehicle battery charging/swap stations in distribution Systems: comparison study and optimal planning," *Power Systems, IEEE Transactions on*, vol. 29, pp. 221-228, 2014.

[28] "A guide to lead-acid batteries", [Online]. Available: www.solar2renewableenergy.com

[29] PJM, www.pjm.com.

[30] A. Khaligh, and Z.H. Li, "Battery, ultracapacitor, fuel cell, and hybrid energy storage systems for electric, hybrid electric, fuel Cell, and pug-In hybrid electric vehicles: state of the art," *IEEE Trans. Veh. Technol.*, vol. 59, no. 6, pp. 2806-2814, Jul. 2010.

[31] Y. Song, Y. Zheng, and D.J. Hill, "Optimal Scheduling for EV Charging Stations in Distribution Networks: A Convexified Model" *IEEE Trans. Power Syst.*, vol. 32, no. 2, Mar. 2017.